Ghost imaging with partially coherent light radiation through turbulent atmosphere

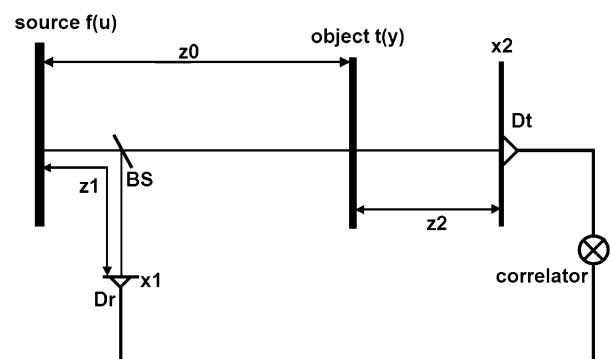## C. Li · T. Wang · J. Pu · W. Zhu · R. Rao

Abstract Based on the classical optical coherent theory and the extended Huygens-Fresnel integral, ghost imaging with partially coherent light radiation through turbulent atmosphere has been studied. The analytical ghost-imaging formulas have been derived. Based on these formulas and the numerical calculation results, we find that the image quality is influenced by the turbulence strength, the propagation distance, and the coherent parameters of the partially coherent light.

1 Introduction

Ghost image is an image of an unknown object from a measurement of the fourth order correlation function. It was firstly realized by using entangled photon pairs generated in spontaneous parametric down-conversion in 1995 [1, 2]. Recently, it was found that the ghost image can be produced with quasi-thermal light [3, 4]. As shown in Fig. 1, a twin beam configuration is used, in which partially coherent light is split into two paths by the beam splitter with an unknown object in the test arm. The final image is reconstructed from the coincidence between the intensities of the two detectors. Neither of the detectors independently produces an image

of the object, but the correlation between the two permits reconstruction of the image.

In recent years, ghost imaging has attracted much interest from investigators and practitioners in the field of quantum optics [5–11]. A very interesting phenomenon of the ghost imaging is that it can be produced without the use of lenses. Some groups have studied the realization of lensless ghost diffraction and its applicability in x-ray diffraction and shown that true images also can be produced from lensless ghost-imaging systems [6–9]. More recently the ghost imaging with fully incoherent source through turbulent atmosphere has been investigated [10]. However, to the best of our knowledge, the investigation of the ghost imaging of partially coherent beam propagating in the turbulent atmosphere has not been published. In this paper, the ghost imaging with partially coherent source propagating in the turbulent atmosphere has been studied. Based on the classical optical coherent theory and the extended Huygens-Fresnel integral, the analytical imaging formula has been obtained. And the influence of turbulence and the beam parameters on the ghost imaging has been discussed.

C. Li · T. Wang · J. Pu (✉)
College of Information Science and Engineering, Huaqiao University, Quanzhou 362021, China
e-mail: jixiong@hqu.edu.cn
Fax: +86-595-22691963

W. Zhu · R. Rao
The Key Laboratory of the Atmospheric Composition and Optical Radiation of Chinese Academy of Sciences, Anhui Institute of Optics and Fine Mechanics, Chinese Academy of Sciences, Hefei, Anhui 230031, China

Fig. 1 Geometry of a lens-less ghost-imaging system through turbulent atmosphere

2 Theory

As shown in Fig. 1, a partially coherent source is split into two beams by the beam splitter. The two beams propagate through two different paths. There is an unknown object located in the test path, and the detector used in this path is a bucket detector. The distance between the source and the object, the source and the reference detector, the object and the test detector are z_0, z_1 and z_2 respectively. A correlator is used to measure the correlation function of the intensity fluctuations.

Based on the classical optical coherent theory, in the one-dimensional case, the correlation function containing the imaging of the object is [12, 13]:

$$g(x_1, x_2) = \langle I_1(x_1) I_2(x_2) \rangle - \langle I_1(x_1) \rangle \langle I_2(x_2) \rangle \quad (1)$$

where I_1 and I_2 denote the intensities in the test and reference beams, respectively. x_1 and x_2 represent two points in the field, respectively. The brackets denote an average over all realizations of the field.

Looking at the reference path, based on the extended Huygens–Fresnel integral [14], the field at D_r is:

$$E_1(x_1) = \left(\frac{-i}{\lambda z_1}\right)^{1/2} \int f(u) e^{\frac{i\pi}{\lambda z_1}(x_1-u)^2} e^{\phi_1(u,x_1)} \, du \quad (2)$$

where $f(u)$ is the source distribution, $\phi_1(u, x_1)$ represents the random part of the complex phase due to the atmospheric turbulence. Similar to the test path, the field at D_t is given by:

$$E_2(x_2) = \left(\frac{-i}{\lambda z_2}\right)^{1/2}\left(\frac{-i}{\lambda z_0}\right)^{1/2} \iint f(u) e^{\frac{i\pi}{\lambda z_0}(y-u)^2}$$
$$\times e^{\phi_0(u,y)} t(y) e^{\frac{i\pi}{\lambda z_2}(x_2-y)^2} e^{\phi_2(x_2,y)} \, du \, dy \quad (3)$$

where $t(y)$ denotes the amplitude of the object. If the statistics of the source and the three propagation regimes are independent, then the intensity correlation can be described as:

$$\langle I_1(x_1) I_2(x_2) \rangle$$
$$= \frac{1}{\lambda^3 z_0 z_1 z_2} \int\int\int\int\int\int \langle f(u_1) f^*(u_1') f(u_2) f^*(u_2') \rangle$$
$$\times \langle e^{\phi_0(u_2,y)+\phi_0^*(u_2',y')} \rangle \langle e^{\phi_1(u_1,x_1)+\phi_1^*(u_1',x_1)} \rangle$$
$$\times \langle e^{\phi_2(x_2,y)+\phi_2^*(x_2',y')} \rangle e^{\frac{i\pi}{\lambda z_0}[(y-u_2)^2-(y'-u_2')^2]}$$
$$\times e^{\frac{i\pi}{\lambda z_1}[(x_1-u_1)^2-(x_1-u_1')^2]} e^{\frac{i\pi}{\lambda z_2}[(x_2-y)^2-(x_2-y')^2]}$$
$$\times t(y) t^*(y') \, du_1 \, du_1' \, du_2 \, du_2' \, dy \, dy'. \quad (4)$$

The last term of (1) can be expressed as:

$$\langle I_1(x_1) \rangle \langle I_2(x_2) \rangle$$
$$= \frac{1}{\lambda^3 z_0 z_1 z_2} \int\int\int\int\int\int \langle f(u_1) f^*(u_1') \rangle \langle f(u_2) f^*(u_2') \rangle$$
$$\times \langle e^{\phi_0(u_2,y)+\phi_0^*(u_2',y')} \rangle \langle e^{\phi_1(u_1,x_1)+\phi_1^*(u_1',x_1)} \rangle$$
$$\times \langle e^{\phi_2(x_2,y)+\phi_2^*(x_2',y')} \rangle e^{\frac{i\pi}{\lambda z_0}[(y-u_2)^2-(y'-u_2')^2]}$$
$$\times e^{\frac{i\pi}{\lambda z_1}[(x_1-u_1)^2-(x_1-u_1')^2]} e^{\frac{i\pi}{\lambda z_2}[(x_2-y)^2-(x_2-y')^2]}$$
$$\times t(y) t^*(y') \, du_1 \, du_1' \, du_2 \, du_2' \, dy \, dy'. \quad (5)$$

It is assumed that the light source be a Gaussian Schell-model one which satisfies Gaussian variate of zero mean, therefore [20]:

$$\langle f(u_1) f^*(u_1') f(u_2) f^*(u_2') \rangle$$
$$= \langle f(u_1) f^*(u_1') \rangle \langle f(u_2) f^*(u_2') \rangle$$
$$+ \langle f(u_1) f^*(u_2') \rangle \langle f(u_2) f^*(u_1') \rangle. \quad (6)$$

Substituting (4), (5) and (6) into (1), we obtain:

$$g(x_1, x_2)$$
$$= \frac{1}{\lambda^3 z_0 z_1 z_2} \int\int\int\int\int\int \langle f(u_1) f^*(u_2') \rangle \langle f(u_2) f^*(u_1') \rangle$$
$$\times \langle e^{\phi_0(u_2,y)+\phi_0^*(u_2',y')} \rangle \langle e^{\phi_1(u_1,x_1)+\phi_1^*(u_1',x_1)} \rangle$$
$$\times \langle e^{\phi_2(x_2,y)+\phi_2^*(x_2',y')} \rangle e^{\frac{i\pi}{\lambda z_0}[(y-u_2)^2-(y'-u_2')^2]}$$
$$\times e^{\frac{i\pi}{\lambda z_1}[(x_1-u_1)^2-(x_1-u_1')^2]} e^{\frac{i\pi}{\lambda z_2}[(x_2-y)^2-(x_2-y')^2]}$$
$$\times t(y) t^*(y') \, du_1 \, du_1' \, du_2 \, du_2' \, dy \, dy'. \quad (7)$$

The first order correlation function in the source plane can be expressed by [11, 15]:

$$\langle f(u_1) f^*(u_2) \rangle = G_0 \exp\left[\frac{u_1^2 + u_2^2}{-4\sigma_l^2} + \frac{(u_1 - u_2)^2}{-2\sigma_g^2}\right] \quad (8)$$

where G_0 is a constant, and is set to be unity in the following text. σ_l represents the source's transverse size, and σ_g represents the source's transverse coherent width.

It is well known that the statistical averages coursed by the turbulent atmosphere can be described approximately by [16–18]:

$$\langle e^{\phi_i(x,y)+\phi_i^*(x',y')} \rangle$$
$$= \exp\left\{\frac{(x-x')^2 + (x-x')(y-y') + (y-y')^2}{-\rho_i^2}\right\} \quad (9)$$

where $\rho_i = (0.55 C_n^2 k z_i)^{-3/5}$ is the coherence length of a spherical wave propagation through a turbulent medium and C_n^2 is the refractive-index structure parameter describing the strength of the atmospheric turbulence in the path z_i.

By using the following equation

$$\int_{-\infty}^{\infty} \exp(-p^2 x^2 \pm qx)\, dx = \exp\left(\frac{q^2}{4p^2}\right) \frac{\sqrt{\pi}}{p}. \qquad (10)$$

Equation (7) can be simplified as

$$
\begin{aligned}
&g(x_1, x_2) \\
&= \frac{G_0^3 \pi^2}{\lambda^3 z_0 z_1 z_2 \sqrt{B_1 B_2 B_3 B_4}} \iint t(y) t^*(y') \\
&\quad \times \exp\left\{ \frac{(y-y')^2}{-\rho_0^2} + \frac{(y-y')^2}{-\rho_2^2} \right. \\
&\quad + \frac{i\pi}{\lambda z_0}(y^2 - y'^2) - \frac{\pi^2 x_1^2}{B_1 \lambda^2 z_1^2} + \frac{A_4^2}{4B_4} \\
&\quad + \frac{i\pi}{\lambda z_2}\left[(x_2 - y)^2 - (x_2 - y')^2 \right] + \frac{\left(\frac{2i\pi x_1}{\lambda z_1} - \frac{2i\pi x_1}{B_1 \rho_1^2 \lambda z_2}\right)^2}{4B_2} \\
&\quad + \left. \frac{\left(\frac{i\pi x_1}{\lambda z_1 B_2 \sigma_g^2} - \frac{y-y'}{\rho_0^2} - \frac{2i\pi y}{\lambda z_0} - \frac{i\pi x_1}{B_1 B_2 \rho_1^2 \lambda z_1 \sigma_g^2}\right)}{4B_3} \right\} dy\, dy'
\end{aligned}
$$

$$(11)$$

where

$$B_1 = \frac{1}{4\sigma_l^2} + \frac{1}{2\sigma_g^2} + \frac{1}{\rho_0^2} - \frac{i\pi}{\lambda z_0},$$

$$B_2 = \frac{1}{4\sigma_l^2} + \frac{1}{2\sigma_g^2} + \frac{1}{\rho_0^2} + \frac{i\pi}{\lambda z_0} - \frac{1}{B_1 \rho_1^4},$$

$$B_3 = \frac{1}{4\sigma_l^2} + \frac{1}{2\sigma_g^2} + \frac{1}{\rho_0^2} - \frac{i\pi}{\lambda z_0} - \frac{1}{4B_2 \sigma_g^4},$$

$$
\begin{aligned}
B_4 &= \frac{1}{4\sigma_l^2} + \frac{1}{2\sigma_g^2} + \frac{1}{\rho_0^2} + \frac{i\pi}{\lambda z_0} - \frac{1}{4B_1 \sigma_g^4} \\
&\quad - \frac{1}{4B_1^2 B_2 \rho_1^4 \sigma_g^4} - \frac{\left(\frac{2}{\rho_0^2} + \frac{1}{2B_1 B_2 \rho_1^2 \sigma_g^4}\right)^2}{4B_3},
\end{aligned}
$$

$$
\begin{aligned}
A_4 &= \frac{y-y'}{\rho_0^2} + \frac{2i\pi y'}{\lambda z_0} - \frac{i\pi x_1}{B_1 \sigma_g^2 \lambda z_1} + \frac{\frac{i\pi x_1}{\lambda z_1} - \frac{i\pi x_1}{B_1 \rho_1^2 \lambda z_2}}{B_1 B_2 \sigma_g^2 \rho_1^2} \\
&\quad + \left(\frac{1}{2B_3 \rho_0^2} + \frac{1}{8B_1 B_2 B_3 \rho_1^2 \sigma_g^4} \right)\left(\frac{i\pi x_1}{B_2 \sigma_g^2 \lambda z_1} - \frac{y-y'}{\rho_0^2} \right. \\
&\quad \left. - \frac{2i\pi y}{\lambda z_0} - \frac{i\pi x_1}{B_1 B_2 \rho_1^2 \lambda z_1 \sigma_g^2} \right).
\end{aligned}
$$

After assuming the test detector as a bucket detector, then the ghost image is proportional to

$$G(x_1) = \int g(x_1, x_2)\, d(x_2)\, dx_2 \qquad (12)$$

where $d(x_2)$ is a detector function introduced to describe the detector [19]; $d(x_2) = 1$, if x_2 is inside D_t or $d(x_2) = 0$. In particular, if the size of D_t is large enough, we can take $d(x_2) = 1$ everywhere. And then $D\left(\frac{y-y'}{\lambda z_2}\right) = \delta\left(\frac{y-y'}{\lambda z_2}\right)$, where $D\left(\frac{y-y'}{\lambda z_2}\right)$ is the Fourier transform of $d(x_2)$. Therefore, (12) can be simplified as

$$
\begin{aligned}
G(x_1) &= \frac{G_0^3 \pi}{2\lambda^2 z_0 z_1 \sqrt{B_1 B_2 B_3 B_4}} \int |t(y)|^2 \exp\left\{ -\frac{\pi^2 x_1^2}{B_1 \lambda^2 z_1^2} + \frac{\left(\frac{2i\pi x_1}{\lambda z_1} - \frac{2i\pi x_1}{B_1 \rho_1^2 \lambda z_2}\right)^2}{4B_2} + \frac{\left(\frac{i\pi x_1}{\lambda z_1 B_2 \sigma_g^2} - \frac{2i\pi y}{\lambda z_0} - \frac{i\pi x_1}{B_1 B_2 \rho_1^2 \lambda z_1 \sigma_g^2}\right)}{4B_3} \right. \\
&\quad + \left. \frac{\left[\frac{2i\pi y}{\lambda z_0} - \frac{i\pi x_1}{B_1 \sigma_g^2 \lambda z_1} + \frac{\frac{i\pi x_1}{\lambda z_1} - \frac{i\pi x_1}{B_1 \rho_1^2 \lambda z_2}}{B_1 B_2 \sigma_g^2 \rho_1^2} + \left(\frac{1}{2B_3 \rho_0^2} + \frac{1}{8B_1 B_2 B_3 \rho_1^2 \sigma_g^4}\right)\left(\frac{i\pi x_1}{B_2 \sigma_g^2 \lambda z_1} - \frac{2i\pi y}{\lambda z_0} - \frac{i\pi x_1}{B_1 B_2 \rho_1^2 \lambda z_1 \sigma_g^2}\right)\right]^2}{4B_4} \right\} dy
\end{aligned}
$$

$$= \frac{\pi}{\lambda^2 z^2} \int |t(y)|^2 h(y, x_1)\, dy \qquad (13)$$

where we have assumed $z_0 = z_1 = z$, and

$$
\begin{aligned}
h(y, x_1) &= \frac{G_0^3}{2\sqrt{B_1 B_2 B_3 B_4}} \exp\left\{ -\frac{\pi^2 x_1^2}{B_1 \lambda^2 z^2} + \frac{\left(\frac{2i\pi x_1}{\lambda z} - \frac{2i\pi x_1}{B_1 \rho_1^2 \lambda z_2}\right)^2}{4B_2} + \frac{\left(\frac{i\pi x_1}{\lambda z_1 B_2 \sigma_g^2} - \frac{2i\pi y}{\lambda z} - \frac{i\pi x_1}{B_1 B_2 \rho_1^2 \lambda z \sigma_g^2}\right)}{4B_3} \right. \\
&\quad + \left. \frac{\left[\frac{2i\pi y}{\lambda z} - \frac{i\pi x_1}{B_1 \sigma_g^2 \lambda z} + \frac{\frac{i\pi x_1}{\lambda z} - \frac{i\pi x_1}{B_1 \rho_1^2 \lambda z_2}}{B_1 B_2 \sigma_g^2 \rho_1^2} + \left(\frac{1}{2B_3 \rho_0^2} + \frac{1}{8B_1 B_2 B_3 \rho_1^2 \sigma_g^4}\right)\left(\frac{i\pi x_1}{B_2 \sigma_g^2 \lambda z} - \frac{2i\pi y}{\lambda z} - \frac{i\pi x_1}{B_1 B_2 \rho_1^2 \lambda z \sigma_g^2}\right)\right]^2}{4B_4} \right\}
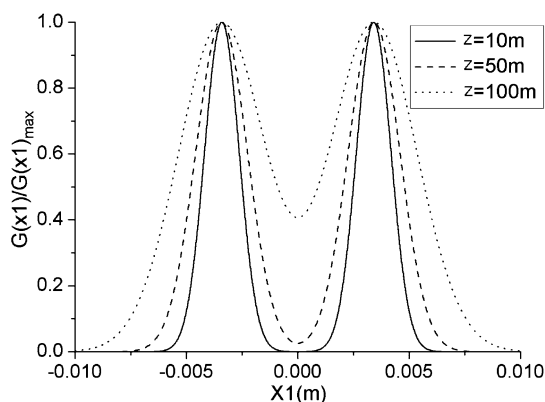\end{aligned}
$$

$$(14)$$

here $h(y, x_1)$ can be regarded as a function of the lens-less ghost-imaging system considering a partially coherent light radiation in the atmospheric turbulence.

Equations (13) and (14) are the main results of this paper. Based on these formulas, we can study the ghost imaging with partially coherent light radiation through turbulent atmosphere. In the next Section, we will give some numerical results to show the image quality influenced by the turbulence strength, the propagation distance, and the coherent parameters of the partially coherent light.

3 Numerical results

To get a clear ghost imaging, we assume that the lens-less ghost-imaging system satisfy the following relation $z_0 = z_1 = z$. The object used in test path is a double slit with 1 mm slit width and 6 mm separation. We made a comparison with different z as shown in Fig. 2. The parameters for calculation are chosen as: $\sigma_l = 5 \times 10^{-3}$ m, $\sigma_g = 1 \times 10^{-3}$ m, $\lambda = 785 \times 10^{-9}$ m, $C_n^2 = 10^{-14}$ m$^{-2/3}$, $z_2 = 50$ m. The object is located at $z = 10, 50, 100$ m, respectively. A high quality ghost imaging can be obtained when the propagation length is short. However, the quality of the ghost image decreases as increasing of the propagation distance z. When the distance is large enough, the image we get is a Gaussian shape.

To investigate the influence of the atmospheric turbulence on the ghost imaging, we change C_n^2 from strong turbulence (10^{-11} m$^{-2/3}$) to weak turbulence (10^{-14} m$^{-2/3}$), shown in Fig. 3. The other parameters for calculation are $\sigma_l = 5 \times 10^{-3}$ m, $\sigma_g = 1 \times 10^{-3}$ m, $\lambda = 785 \times 10^{-9}$ m, $z = 30$ m, $z_2 = 50$ m. From Fig. 3, we can directly see that the ghost imaging becomes better while the turbulence becomes weaker, and the atmospheric turbulence seems having little influence on the imaging when C_n^2 is weaker than 10^{-14} m$^{-2/3}$.
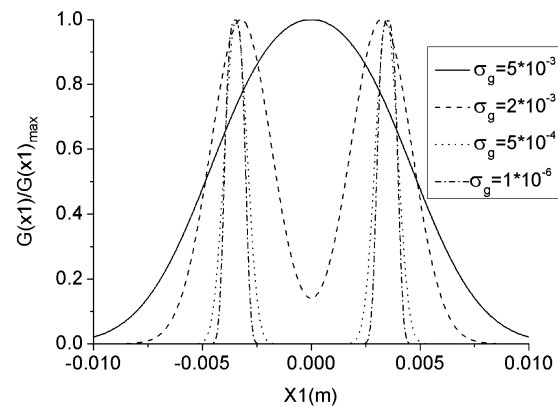
In Fig. 4, we have studied the influence of the source's transverse coherent width on the ghost imaging. The para-
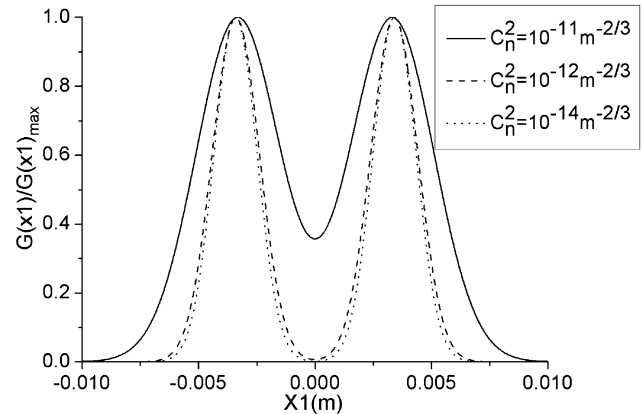
Fig. 3 The ghost imaging of a double slit with partially coherent source for different C_n^2. The other parameters are: $\sigma_l = 5 \times 10^{-3}$ m, $\sigma_g = 1 \times 10^{-3}$ m, $\lambda = 785 \times 10^{-9}$ m, $z = 30$ m, $z_2 = 50$ m


Fig. 4 The ghost imaging of a double slit with partially coherent source for different σ_g. The other parameters are: $\sigma_l = 5 \times 10^{-3}$ m, $\lambda = 785 \times 10^{-9}$ m, $z = 10$ m, $z_2 = 50$ m, $C_n^2 = 10^{-14}$ m$^{-2/3}$

Fig. 2 The ghost imaging of a double slit with partially coherent source for different z. The other parameters are: $\sigma_l = 5 \times 10^{-3}$ m, $\sigma_g = 1 \times 10^{-3}$ m, $\lambda = 785 \times 10^{-9}$ m, $C_n^2 = 10^{-14}$ m$^{-2/3}$, $z_2 = 50$ m
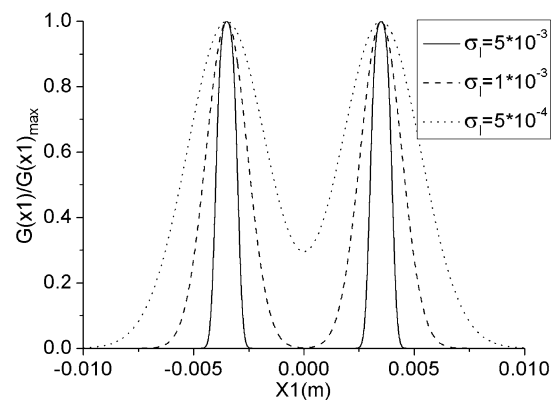
Fig. 5 The ghost imaging of a double slit with partially coherent source for different σ_l. The other parameters are $\sigma_g = 5 \times 10^{-6}$ m, $\lambda = 785 \times 10^{-9}$ m, $z = 10$ m, $z_2 = 50$ m, $C_n^2 = 10^{-14}$ m$^{-2/3}$

Fig. 6 The ghost imaging of a double slit with partially coherent source for different z_2. The other parameters are:
$\sigma_l = 5 \times 10^{-3}$ m,
$\sigma_g = 1 \times 10^{-3}$ m,
$\lambda = 785 \times 10^{-9}$ m,
$C_n^2 = 10^{-14}$ m$^{-2/3}$, $z = 30$ m
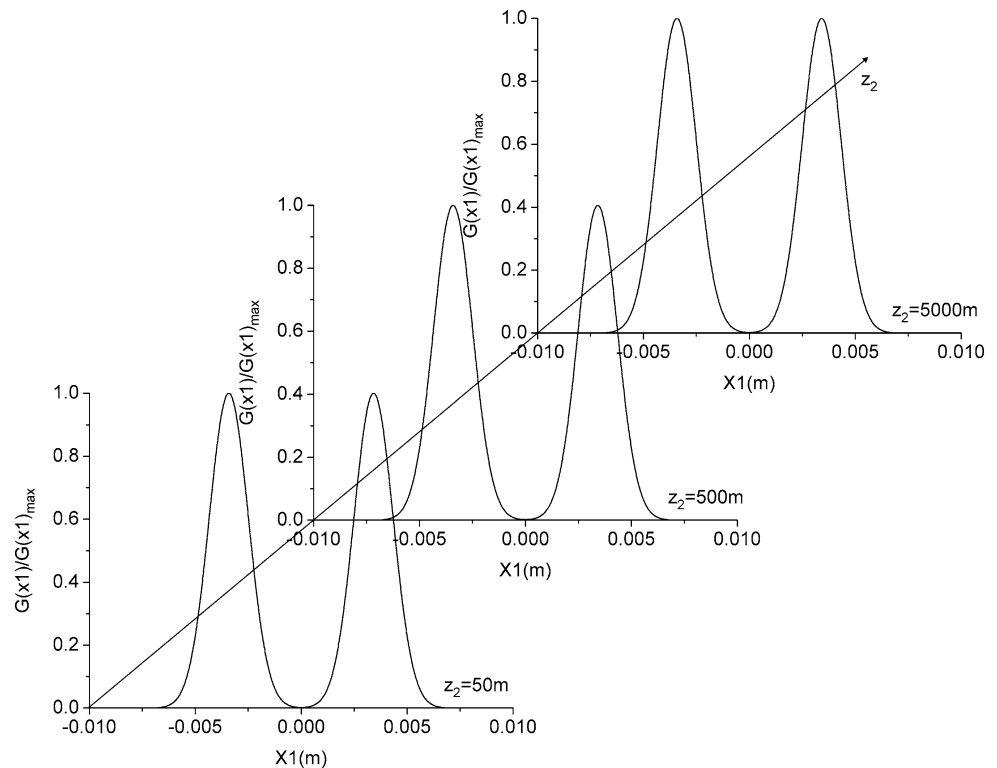
meters for Fig. 4 are $\sigma_l = 5 \times 10^{-3}$ m, $\lambda = 785 \times 10^{-9}$ m, $z = 10$ m, $z_2 = 50$ m, $C_n^2 = 10^{-14}$ m$^{-2/3}$. The source's transverse coherent width is set as $\sigma_g = 5 \times 10^{-3}$, 2×10^{-3}, 5×10^{-4}, 1×10^{-6} m respectively. We can find that with the increasing of σ_g, the quality of the ghost imaging decreases and the imaging will finally become of a Gaussian shape. The source can be regards as incoherence source when σ_g is small enough, such as 1×10^{-6} m.

Finally, the influence of the source's transverse size on the ghost imaging have been studied as shown in Fig. 5. The parameters for calculation are $\sigma_g = 5 \times 10^{-6}$ m, $\lambda = 785 \times 10^{-9}$ m, $z = 10$ m, $z_2 = 50$ m, $C_n^2 = 10^{-14}$ m$^{-2/3}$. The source's transverse size is chosen as $\sigma_l = 5 \times 10^{-3}$, 1×10^{-3}, 5×10^{-4} m respectively. From Fig. 5, we can find that the quality of the ghost imaging becomes better with the increase of σ_l.

What we have to point out is that the distance between the object and the test detector z_2 seems to have little influence on the ghost imaging as shown in Fig. 6. The parameters are chosen as: $\sigma_l = 5 \times 10^{-3}$ m, $\sigma_g = 1 \times 10^{-3}$ m, $\lambda = 785 \times 10^{-9}$ m, $C_n^2 = 10^{-14}$ m$^{-2/3}$, $z = 30$ m.

4 Conclusions

Ghost imaging can be produced with partially coherent light propagating through turbulent atmosphere. Based on the classical optical coherent theory and the extended Huygens-Fresnel integral, we obtained an analytical imaging formula.

The influence of the turbulence strength, propagation length, the source's transverse size and coherent width on the quality of the ghost imaging has been discussed. The larger the source's transverse size is, the better the quality of the ghost imaging. When the turbulence strength, propagation length and the source's coherent width increase, the quality of the ghost imaging decreases and the image will finally become of a Gaussian shape. But the distance between the unknown object and the detector has little influence on the ghost imaging.

References

1. T.B. Pittman, Y.H. Shin, D.V. Strekalov, A.V. Sergienko, Phys. Rev. A **52**, R3429 (1995)
2. D.V. Strekalov, A.V. Sergienko, D.N. Klyshko, Y.H. Shin, Phys. Rev. Lett. **74**, 3600 (1995)
3. A. Valencia, G. Scarcelli, M.D. Angelo, Y. Shih, Phys. Rev. Lett. **94**, 063601 (2005)
4. D. Magatti, F. Ferri, A. Gatti, M. Bache, E. Brambilla, L.A. Lugiato, Phys. Rev. Lett. **94**, 183602 (2005)
5. A. Gatti, M. Bache, D. Magatti, E. Brambilla, F. Ferri, L.A. Lugiato, J. Mod. Opt. **53**, 739 (2006)
6. J. Cheng, S. Han, Phys. Rev. Lett. **92**, 093903 (2004)

7. M.H. Zhang, Q. Wei, X. Shen, Y.F. Liu, H.L. Liu, J. Cheng, S.S. Han, Phys. Rev. A **75**, 021803 (2007)
8. G. Scarcelli, V. Berardi, Y. Shih, Appl. Phys. Lett. **88**, 061106 (2006)
9. L. Basano, P. Ottonello, Appl. Phys. Lett. **89**, 091109 (2006)
10. J. Cheng, Opt. Express **17**, 7916 (2009)
11. Y.J. Cai, S.Y. Zhu, Phys. Rev. E **71**, 056607 (2005)
12. A. Gatti, E. Brambilla, M. Bache, L.A. Lugiato, Phys. Rev. Lett. **93**, 093602 (2004)
13. A. Gatti, E. Brvambilla, M. Bache, L.A. Lugiato, Phys. Rev. A **70**, 013802 (2004)
14. J.C. Ricklin, F.M. Davidson, J. Opt. Soc. Am. A **19**, 1794 (2002)
15. J.T. Foley, M.S. Zubairy, Opt. Commun. **26**, 297 (1976)
16. J.H. Li, B.D. Lu, J. Opt. A, Pure Appl. Opt. **11**, 075401 (2009)
17. X.L. Ji, X.Q. Li, J. Opt. Soc. Am. A **26**, 236 (2009)
18. H.T. Eyyuboğlu, Y. Baykal, Opt. Express **12**, 4659 (2004)
19. J. Cheng, Phys. Rev. A **78**, 043823 (2008)
20. L. Mandel, E. Wolf, *Optical Coherence and Quantum Optics* (Cambridge University Press, Cambridge, 1995)